CALCULATION OF A SUPERSONIC JET EMERGING FROM A HOLE WITH PLANAR WALLS

V. N. Kamzolov and U. G. Pirumov

Zhurnal Prikladnoi Mekhaniki i Tekhnicheskoi Fiziki, Vol. 8, No. 2, pp. 117-122, 1967

ABSTRACT: The coordinates of the sonic line are derived by means of Frankl's solution [1], while the supersonic part of the jet is considered by the method of characteristics. The numerical solution has been used to calculate the family of rarefaction waves and a family of nozzles having a corner point and a curvilinear transition surface. These calculations show that, when there is a corner point, the shape of the sonic line has hardly any effect on the velocity distribution along the symmetry axis. It is also shown that a positive pressure gradient arises on the surface of the nozzle beyond the corner point if that point lies upstream from the limiting characteristic of the first family.

A comparison is made with the approximate transonic solution [2, 3] near the center of the nozzle. We are indebted to G. K. Bunina for assistance with the calculations.

§1. Sonic line. Frankl [1] gave a solution for this type of jet. The shape of the sonic line and the velocity at the wall are derived for a planar hole whose walls are inclined at an angle $\theta_0 = \pi/2$ to the x-axis.

The formula [1] for the function ψ is

$$\psi = -\theta/\pi + a_0\psi^\circ + \delta\psi\,, \tag{1.1}$$

$$\psi^\circ = \sum_{n=1}^{\infty} \frac{z_n(\tau)}{z_n(\tau_*)}\,\frac{\sin 2n\theta}{n^{4/3}}\,, \tag{1.2}$$

$$\delta\psi = \sum_{n=1}^{\infty} a_n \frac{z_n(\tau)}{z_n(\tau_*)} \sin 2\,n\theta\,, \tag{1.3}$$

in which θ is the inclination of the velocity to the x-axis, τ is the square of the ratio of the velocity to the velocity of flow into a vacuum, and τ_* is the value of τ at the sonic point.

In deriving the coefficients of (1.3) from the boundary conditions, Frankl calculated only the first four coefficients. Formula (1.3) is used to determine the coordinates of the sonic line and the inclination of the velocity on it. The values of ψ are used to determine the coordinates of the sonic line via Chaplygin's equations and the formulas for passing from the physical plane to the hodograph plane [4]. Some simple steps give

$$x(\theta) = 3.864\Big[-\int_0^{1/2\pi}\Big(\psi + \frac{\partial\psi}{\partial\tau}\Big)\cos\theta\, d\theta + \int_0^{\theta}\Big(\psi + \frac{\partial\psi}{\partial\tau}\Big)\cos\theta d\theta - \frac{1}{2} - \psi\sin\theta\Big],$$

$$y(\theta) = 3.864\Big[\int_0^{\theta}\Big(\psi + \frac{\partial\psi}{\partial\tau}\Big)\sin\theta d\theta + \psi\cos\theta\Big]. \tag{1.4}$$

Formulas allowing one to sum the series of (1.2) for $\tau = \tau_*$ have been used in calculating ψ and $\partial\psi/\partial\tau$, namely

$$\Gamma(\alpha)\sum \frac{e^{ni\varphi}}{n^\alpha} = \int_0^\infty \frac{x^{\alpha-1}dx}{e^{x-i\varphi}-1} \qquad (\alpha > 0),$$

in which $\Gamma(\alpha)$ is the gamma function, and also asymptotic formulas for $z_n'(\tau)$ for $\tau = \tau_*$ [1]:

$$\frac{\tau^*}{n}\cdot\frac{z_n'(\tau_*)}{z_n(\tau_*)} = -\frac{1}{2}\Big(\frac{2}{\gamma+1}\Big)^{\frac{1}{\gamma-1}}(C_0 n^{-1/3} + C_1 n^{-1} + C_2 n^{-5/3} + C_3 n^{-7/3})\,, \tag{1.5}$$

in which $C_0 = -2.444$, $C_1 = 1.2305$, $C_2 = -0.6478$, and $C_3 = 0.23779$, and γ is the ratio of the specific heats. The results for ψ and $\partial\psi/\partial\tau$ are as follows:

$$\psi = -\frac{\theta}{\pi} + \sum_1^3 a_n \sin 2n\theta + \frac{a_0\sin 2\theta}{\Gamma(4/3)}A\,,$$

$$2\tau_*\frac{\partial\psi}{\partial\tau} = -\Big(\frac{2}{\gamma+1}\Big)^{\frac{1}{\gamma-1}}\Big\{\Big[\frac{C_0}{\Gamma(2/3)}B + \frac{C_1}{\Gamma(4/3)}A + \frac{C_2}{\Gamma(2)}C + \frac{C_3}{\Gamma(4/3)}D\Big]a_0\sin 2\theta +$$

x	y	θ (rad)	ψ	$2\tau_*\,\partial\psi/\partial\tau$
0.8361	0	0	0	0
0.8360	0.04863	−0.001091	0.0256	0.2814
0.8347	0.1200	−0.002041	0.04602	1.405
0.8309	0.2012	−0.002182	0.05207	2.031
0.8218	0.2730	−0.003272	0.07064	2.314
0.8123	0.3264	−0.004363	0.08445	2.300
0.7788	0.4486	−0.008727	0.11603	1.8006
0.7517	0.5208	−0.01309	0.1346	1.5249
0.7283	0.5759	−0.017453	0.1488	1.3639
0.6878	0.6611	−0.02618	0.1706	1.1650
0.6527	0.7276	−0.03491	0.1875	0.0387
0.6215	0.7832	−0.04363	0.2016	0.9480
0.5930	0.8313	−0.05236	0.2137	0.8783
0.5667	0.8742	−0.06109	0.2243	0.8222
0.5423	0.9130	−0.06981	0.2389	0.7756
0.5194	0.9485	−0.07854	0.2427	0.7361
0.4875	0.9970	−0.09163	0.2545	0.6863
0.4580	1.0410	−0.1047	0.2651	0.6449
0.4219	1.0942	−0.1222	0.2777	0.5990
0.3511	1.1973	−0.1614	0.3016	0.5211
0.2975	1.2758	−0.1963	0.3191	0.4698
0.2143	1.4012	−0.2618	0.3458	0.3992
0.1365	1.5272	−0.3403	0.3710	0.3393
0.05665	1.6735	−0.4494	0.3981	0.2797
−0.04028	1.9075	−0.6763	0.4364	0.1955
−0.07395	2.0384	−0.8508	0.4550	0.1455
−0.08343	2.130	−1.0167	0.4673	0.1032
0	2.256	−1.5708	0.5	0

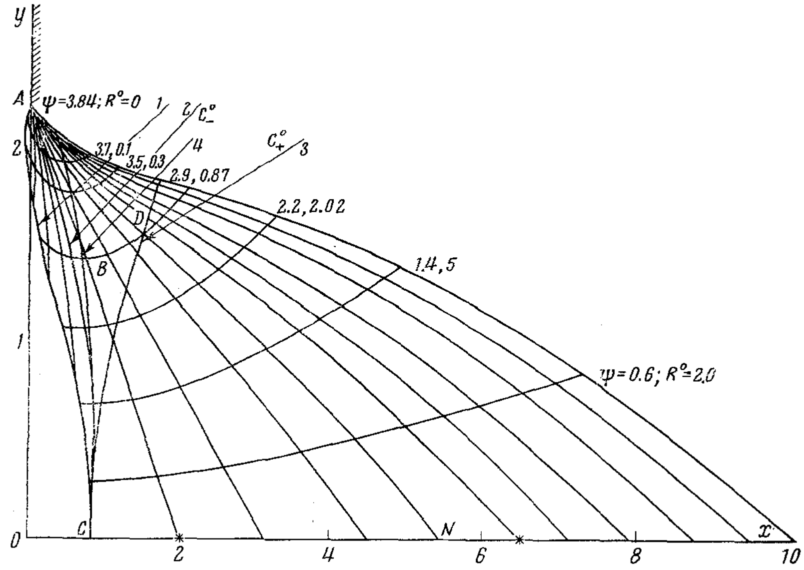

Fig. 1

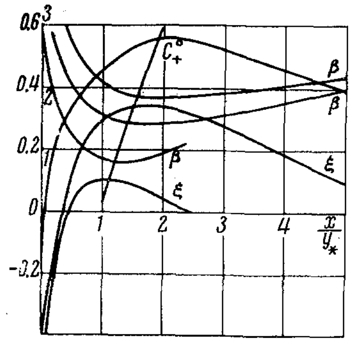

Fig. 2

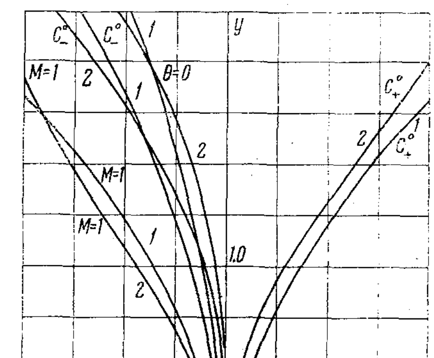

Fig. 3

$$+\sum_{n=1}^{3} a_n \sin 2n\theta \left[C_0 n^{-1/3} + C_1 n^{-1} + C_2 n^{-5/3} + C_3 n^{-7/3}\right]\Big\},$$

$$A = \int_0^\infty \frac{x^{1/3}\,dx}{e^x + e^{-x} - 2\cos 2\theta},$$

$$B = \int_0^\infty \frac{{}^3/_2\,(e^x - e^{-x})\,x^{2/3}\,dx}{(e^x - 2\cos 2\theta + e^{-x})^2},$$

$$C = \int_0^\infty \frac{x\,dx}{e^x + e^{-x} - 2\cos 2\theta},$$

$$D = \int_0^\infty \frac{x^{5/3}\,dx}{e^x + e^{-x} - 2\cos 2\theta}.$$

An M-20 computer was used to calculate the coordinates of the sonic line, the inclination of the velocity at that line, and ψ and $2\tau_* d\psi/d\tau$ for a planar hole with $\theta_0 = \pi/2$ (see table).

A quantity of interest is $d\lambda/dx$, in which λ is the velocity coefficient, at the center of the nozzle. The relations between the physical plane and the hodograph plane [4] give

$$dx = -\frac{1}{2\tau\sqrt{\tau}}\left(1 - \frac{\gamma+1}{\gamma-1}\tau\right)(1-\tau)^{-\frac{1}{\gamma-1}}\frac{\partial\psi}{\partial\theta}\,d\tau,$$

$$\left.\frac{\partial\psi}{\partial\theta}\right|_{\theta=0} = -\frac{1}{\pi} + 2n\sum_{n=1}^{3} a_n \frac{z(\tau)}{z(\tau^*)} + 2a_0\sigma,$$

$$\sigma = \sum_{n=1}^{\infty} \frac{z_n(\tau)}{z_n(\tau_*)}\frac{1}{n^{1/3}}.$$

Here

$$\left(1 - \frac{\gamma+1}{\gamma-1}\tau\right) \to 0, \qquad \frac{\partial\psi}{\partial\theta} \to \infty \qquad \text{for } \tau \to \tau_*$$

because the series for σ diverges. Simple steps give

$$\left[\left(1 - \frac{\gamma+1}{\gamma-1}\tau\right)\frac{\partial\psi}{\partial\theta}\right]_{\tau\to\tau_*} = \frac{\gamma+1}{\gamma-1}\frac{\sigma^2(\tau_*)}{\sigma'(\tau_*)}.$$

The asymptotic expression of (1.5) for $z_n'(\tau_*)$ is used with the integral representation of the Riemann zeta function and the series representation of that function [5] to give

$$\frac{d\lambda}{dx} = \frac{C_0 y_* [\varepsilon(1)]^2}{3a_0(\gamma+1)\sqrt{\gamma+1/\gamma-1}} = 0.5446,$$

$$\varepsilon(1) = \left(\frac{2}{\gamma+1}\right)^{\frac{1}{\gamma-1}},$$

in which $2y_*$ is the width of the hole. The radius of curvature of the streamline at the point of intersection with the sonic line can be determined from

$$R = \frac{\cos^2\theta\,(1+\mathrm{tg}^2\,\theta)^{3/2}}{d\theta/dx}, \qquad \frac{dx}{d\theta} = \sqrt{6}\,\frac{2\tau_*}{\varepsilon(1)}\frac{d\psi}{d\tau}\cos\theta.$$

§2. Supersonic part. This flow was calculated by the method of characteristics [6] with the M-20 computer. This gave the limiting characteristics C_+° and C_-° of the first and second families, the line $\theta = 0$, and ten intermediate lines. Figure 1 shows the sonic line (curve 1), C_-° (curve 2), C_+° (curve 3), $\theta = 0$ (curve 4), and the rarefaction lines. The streamlines show the relative radii of curvature R° at the sonic point (this relative radius is the ratio of the radius of curvature to the radius of the minimum cross-section for that line), as well as the flow corresponding to that line and referred to $0.5\,\rho_* a_*$ (at $\psi = 3.864$).

The flow parameters change monotonically along C_-°, namely M and the modulus of the inclination of the velocity increase with y. M and that inclination change similarly on all characteristics of the second family that start from the nodal point and run to the sonic line up the flow from C_-°. The characteristics of the second family that start from the nodal point and run down the flow from C_-° do not have monotonic variation in M and the inclination (Fig. 2); M decreases from the nodal point to the point of intersection with the C_+° characteristic, but increases from the point of intersection to the axis, while the angle increases from the corner point to the point of intersection but thereafter falls to zero. In Fig. 2, $\beta = (M^2 - 1)^{1/2}$, $\xi = \tan\theta$.

This behavior is readily explained from the conditions of compatibility on the characteristics. Let $\nu(M)$ be the Prandtl-Meyer number; then (Fig. 1) on ADN

$$\nu(M) + \theta = \nu(M_N),$$

at A

$$\nu(M_A) - \theta_A = {}^1/_2\,\pi, \quad \text{or} \quad \nu(M_A) = {}^1/_2\,\nu(M_N) + {}^1/_4\,\pi,$$

on C_+°

$$\nu(\dot{M}) - \theta = 0,$$

at D (intersection of ADN and C_+°)

$$\nu(M_D) = {}^1/_2\nu(M_N).$$

These relationships imply that

$$M_D < M_N, \qquad M_A > M_D.$$

It can be shown that M decreases monotonically on part AD of ADN, and increases monotonically on part DN. From

$$\nu(M) + \theta = \nu(M_N),$$

it follows that θ is also not monotonic on ADN.

§3. Comparison with approximate solution. The approximate equation for transonic flow in the planar case is [2]

$$-(\gamma+1)\,\Phi_{xx}\Phi_x + \Phi_{yy} = 0.$$

In deriving this it has been assumed that the speed of the gas is close to the speed of sound, while the angle between the velocity vector and the x-axis is small. The exact solution to this equation is the first term of Meyer's series near the center of the nozzle and takes the form

$$\Phi = {}^1/_2\,\alpha\,x^2 + {}^1/_2\,(\gamma+1)\,\alpha^2\,xy^2 + {}^1/_{24}\,(\gamma+1)^2\,\alpha^3 y^4,$$

in which $\alpha = dw/dx$ at the center. This gives us the velocity components u and v parallel and perpendicular to the axis as

$$u/a^* = 1 + \alpha x + {}^1/_2\,(\gamma+1)\,\alpha^2 y^2 + \ldots,$$

$$v/a_* = (\gamma+1)\,\alpha^2 xy + {}^1/_6\,(\gamma+1)^2\,\alpha^3 y^3 + \ldots.$$

These formulas allow us to calculate the shape of the sonic line, the line, $\theta = 0$, and of C_-° and C_+°. The first three are

$$x = -{}^1/_2\,(\gamma+1)\,\alpha y^2, \qquad x = {}^1/_6\,(\gamma+1)\,\alpha y^2, \qquad \theta = 0,$$

while the latter two are

$$x = -{}^1/_4\,(\gamma+1)\,\alpha y^2, \qquad x = {}^1/_2\,(\gamma+1)\,\alpha y^2.$$

Figures 3 and 4 give some results from comparison of the exact and approximate solutions. Figure 3 gives the coordinates of the sonic line, the line $\theta = 0$, and also C_+° and C_-°, while Fig. 4 shows θ as a function of y. In these figures, curve 1 corresponds to the approximate solution, while curve 2 corresponds to the present numerical solution. The discrepancies are only 10–20% up to $y \approx 2$ for the coordinates of the sonic line, the line $\theta = 0$, and also C_+° and C_-°; but the θ for $y \leq 0.9$ (which corresponds to $R^\circ \geq 4$) and the modulus of the velocity on the sonic line and the line $\theta = 0$ differ by a factor 2 (Fig. 4). The approximate formulas are therefore unsuitable for flow in nozzles in cases of practical interest with $R^\circ \leq 4$; they are applicable only when the flow near the critical section differs only slightly from one-dimensional, as was assumed in deducing the approximate equation for the potential of the transonic flow.

§4. Curvilinear transition and streamline point. Each corner can serve as the contour of a nozzle, starting from the subsonic region. It

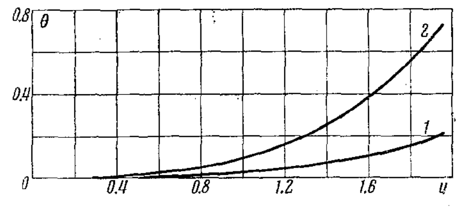

Fig. 4

is of interest to use the transonic parts to derive the supersonic part with a corner point and with a uniform flow parallel to the axis. It is usual in calculating the supersonic part of a nozzle with a corner point to assume that the sonic line is straight and that the velocity on it is parallel to the axis [7], as there is no exact solution for transonic flow with a curvilinear transition surface. Then the rarefaction lines arising from flow past the corner point are calculated. A given M is assumed, and a characteristic with a uniform flow parallel to the axis is taken to solve the Gurs problem and to define the supersonic part of the nozzle with a corner point. In our case, we have located the corner point at various points on the line $\theta = 0$, which correspond to stream lines with different R°. Rarefaction waves were calculated for these various positions. Figure 5 shows the distribution of M along the axis of the nozzle for various R° (x° is the ratio of the distance from the corner point to the radius of the critical section, in which the corner point lies). The value R° = 0 corresponds to flow from a planar hole with $\theta_0 = \pi/2$, while R° = ∞ corresponds to flow from a planar hole with a rectilinear sonic line. It is clear from Fig. 5 that the axial

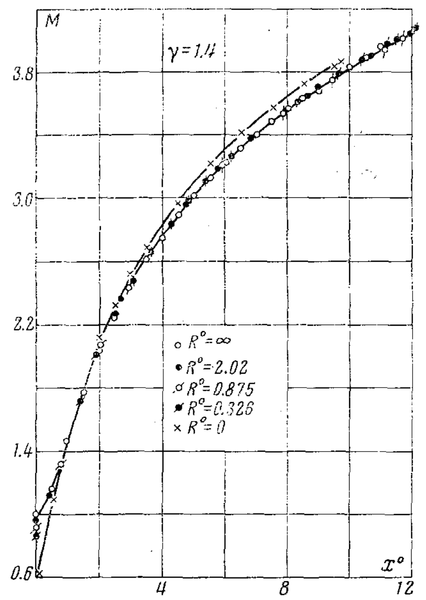

Fig. 5

distribution of M and the acceleration on flow past the corner point are only slightly dependent on the shape of the sonic line. The acceleration is somewhat greater with M > 2 for R° = 0.

These rarefaction waves were used to calculate nozzles with corner points having a uniform flow parallel to the axis for $M_0 \approx 4$, which differed in shape of transition line in the transonic part and hence in R°. Figure 6 shows the distribution of M on the wall. A nozzle with a curvilinear sonic line has a positive pressure gradient near the corner point (minimum in the distribution of M). The pressure gradient decreases as R° increases. There is no positive pressure gradient for a nozzle with a straight sonic line.

This minimum in M is related to the nonmonotonic behavior of M on the rarefaction waves. As the characteristic at the exit from the nozzles is rectilinear, and the parameters on it are constant, all characteristics of the first family are also rectilinear and have constant parameters, so the nonmonotonic parameter variation on the rarefaction-wave characteristics is transferred to the nozzle contour and to all intermediate streamlines lying above the point of intersection of the last characteristic for the waves with the C_+° characteristic. This implies that a positive gradient will be absent in a nozzle with a corner point if the corner point in the transonic region lies downstream from point D in Fig. 1.

Consider the flow for various R° in the transonic part at the point $\theta = 0$. Calculations have been performed for a nozzle with a recti-

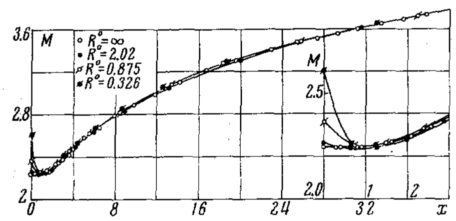

Fig. 6

linear sonic line at the inlet and a uniform flow parallel to the axis at the exit with $M_0 = 4$. The calculations show that here a curvilinear transition surface causes the distribution of M near the corner point to vary with R°, and that there is a positive pressure gradient. However, the distributions of M in the rest of the nozzle are fairly similar, in spite of the differences in the transonic part.

REFERENCES

1. F. I. Frankl, "Flow of a supersonic jet from a vessel with planar walls," Dokl. AN SSSR, **58**, no. 3, 1947.

2. K. G. Guderley, The Theory of Transonic Flow [Russian translation], Izd. Inostr. lit., 1960.

3. R. Sauer, Flow of a Compressible Fluid [Russian translation], Izd. Inostr. lit., 1954.

4. N. E. Kochin, I. A. Kibel, and N. V. Roze, Theoretical Hydromechanics, Part 2 [in Russian], Fizmatgiz, 1963.

5. N. S. Gradshtein and I. M. Ryzhik, Tables of Integrals, Sums, Series, and Products [in Russian], Fizmatgiz, 1963.

6. O. N. Katskova, I. P. Naumova, Yu. D. Shmyglevskii, and N. P. Shulishnina, Computation of Planar and Axially Symmetric Supersonic Gas Flows by the Method of Characteristics [in Russian], VTs AN SSSR, 1961.

7. O. N. Katskova and Yu. D. Shmyglevskii, "Axially symmetric supersonic flow of a freely expanding gas with a planar transition surface," collection: Computational Mathematics [in Russian], Izd. AN SSSR, 1957.

15 July 1966 Moscow